



## H-2-He collisions: Ab initio theory meets cavity-enhanced spectra

Michał Slowinski, Franck Thibault, Yan Tan, Jin Wang, Agnès Pernet-Liu, Shui-Ming Hu, Samir Kassi, Alain Campargue, Magdalena Konefal, Hubert Jóźwiak, et al.

### ► To cite this version:

Michał Slowinski, Franck Thibault, Yan Tan, Jin Wang, Agnès Pernet-Liu, et al.. H-2-He collisions: Ab initio theory meets cavity-enhanced spectra. *Physical Review A*, American Physical Society, 2020, 101 (5), pp.052705. 10.1103/PhysRevA.101.052705 . hal-02886121

HAL Id: hal-02886121

<https://hal.archives-ouvertes.fr/hal-02886121>

Submitted on 9 Jul 2020

**HAL** is a multi-disciplinary open access archive for the deposit and dissemination of scientific research documents, whether they are published or not. The documents may come from teaching and research institutions in France or abroad, or from public or private research centers.

L'archive ouverte pluridisciplinaire **HAL**, est destinée au dépôt et à la diffusion de documents scientifiques de niveau recherche, publiés ou non, émanant des établissements d'enseignement et de recherche français ou étrangers, des laboratoires publics ou privés.

# H<sub>2</sub>-He collisions: *ab initio* theory meets cavity-enhanced spectra

Michał Słowiński,<sup>1,\*</sup> Franck Thibault,<sup>2</sup> Yan Tan,<sup>3</sup> Jin Wang,<sup>3</sup> An-Wen Liu,<sup>3</sup> Shui-Ming Hu,<sup>3</sup> Samir Kassi,<sup>4</sup> Alain Campargue,<sup>4</sup> Magdalena Konefał,<sup>1,4</sup> Hubert Jóźwiak,<sup>1</sup> Konrad Patkowski,<sup>5</sup> Piotr Żuchowski,<sup>1</sup> Roman Ciuryło,<sup>1</sup> Daniel Lisak,<sup>1</sup> and Piotr Wcisło<sup>1,†</sup>

<sup>1</sup> Institute of Physics, Faculty of Physics, Astronomy and Informatics,

Nicolaus Copernicus University in Toruń, Grudziądzka 5, 87-100 Toruń, Poland

<sup>2</sup> Univ Rennes, CNRS, IPR (Institut de Physique de Rennes) - UMR 6251, F-35000 Rennes, France

<sup>3</sup> Hefei National Laboratory for Physical Sciences at Microscale, iChEM,  
University of Science and Technology of China, Hefei, 230026 China

<sup>4</sup> University of Grenoble Alpes, CNRS, LIPhy, F-38000 Grenoble, France

<sup>5</sup> Department of Chemistry and Biochemistry, Auburn University, Auburn, AL 36849 USA

(Dated: April 21, 2020)

Fully quantum *ab initio* calculations of the collision-induced shapes of two rovibrational H<sub>2</sub> lines perturbed by He provide an unprecedented subpercent agreement with ultra-accurate cavity-enhanced measurements. This level of consistency between theory and experiment hinges on a highly accurate potential energy surface and a realistic treatment of the velocity changing and dephasing collisions. In addition to the fundamental importance, these results show that *ab initio* calculations can provide reference data for spectroscopic studies of planet atmospheres at the required accuracy level and can be used to populate spectroscopic line-by-line databases.

## I. INTRODUCTION

Molecular hydrogen differs in many respects from most other diatomic molecules, revealing its nonclassical nature due to a large rotational constant ( $B = 60.853 \text{ cm}^{-1}$ ) [1]. The most straightforward example can be traced back to the early twentieth century, when the heat capacity of H<sub>2</sub> at low temperatures was discovered to dramatically diverge from the expected classical behavior [2]. The lack of inelastic channels in H<sub>2</sub> scattering, up to relatively large temperatures of a few hundred kelvin [3], results in many other atypical features observed in H<sub>2</sub> collision studies. In the particular case of the optically excited H<sub>2</sub> molecule, the lack of inelasticity causes the rate of optical excitation damping to be much smaller than the rate of velocity-changing collisions. This property results in strong collisional Dicke narrowing of the H<sub>2</sub> rovibrational lines [4, 5]. Furthermore, the opening of the first inelastic channel leads to a strong dependence of the generalized spectroscopic cross-section on the collision energy [3], which enhances the speed dependence of the line-shape parameters. Pronounced collisional effects make the molecular hydrogen well suited to study not only the potential energy surfaces (PESs) and quantum-scattering calculation methodology, but also the models describing the collision-perturbed velocity distribution of the optical coherence [3, 6–9], which constitute a long-term development at the frontier of quantum optics, collision theory and statistical physics [10, 11].

Experimental studies on the interactions between two hydrogen molecules and between a hydrogen molecule

and a noble gas atom have a several-decades-long history [6, 7, 12–15]. Recently, the rotationally inelastic scattering of the HD molecule colliding with D<sub>2</sub> [16, 17] and with He [18] at 1 K was observed in coexpanded supersonic beams and theoretically handled by Croft et al. [19]. The influence of the molecular hydrogen collisions, with perturbers such as H<sub>2</sub> isotopologues or noble gas atoms, on the shapes of the rotational and rovibrational lines in H<sub>2</sub> were already established in a wide range of temperatures from 20 K to 1200 K [20–26]. In particular, the effects of the H<sub>2</sub>-He collisions on the widths and shifts of H<sub>2</sub> rovibrational lines were subjected to intense experimental and theoretical studies [3, 25, 27–32]. However, the collision-perturbed line profiles calculated from first principles never reached agreement with experimental data at the subpercent level.

In this work, we report a full *ab initio* description of the collision-perturbed shapes of rovibrational lines for the simplest benchmark system, i.e., He-perturbed H<sub>2</sub>. We demonstrate, for the first time, agreement between measured and *ab initio* computed collision-perturbed shapes of molecular lines at the subpercent level: the root-mean-square difference (calculated within  $\pm \text{FWHM}$ ) between experimental and theoretical profiles is smaller than one-hundredth of the profile amplitude. We merged all of the theoretical tools that are necessary to reach this agreement; i.e., we used the state-of-the-art statistical model of the collision-perturbed shape of molecular lines [33–36], we derived all parameters of this model from quantum scattering calculations [30, 37–39], and we used the highly accurate *ab initio* PES [30, 40], referred to as BSP3. We demonstrate that the fully *ab initio* calculations can provide reference spectra for atmospheric studies of Solar System planets and exoplanets at the required metrological (subpercent) level of accuracy. Therefore, this approach is well-suited for populating line-by-line spec-

\* mslowinski@umk.pl

† piotr.wcislo@fizyka.umk.pl

troscopic databases such as HITRAN [41], GEISA [42], and ExoMol [43], including the recent advanced database structures [44] involving beyond-Voigt line-shape parameters and their wide ranges of temperature representations. We show that this approach can be used to experimentally test the quality of quantum-chemical calculations of the PESs [30, 38, 40, 45, 46].

## II. EXPERIMENTS

To validate our *ab initio* quantum scattering calculations, we performed measurements of the He-perturbed 3-0 S(1) H<sub>2</sub> line centered at 12265.59 cm<sup>-1</sup> (815.33 nm) and the 2-0 Q(1) H<sub>2</sub> line centered at 8075.31 cm<sup>-1</sup> (1238.39 nm) using the experimental setups in Hefei [47] and Grenoble [48–51], respectively. Both setups as seen in Fig. 1, are based on continuous-wave laser sources and high-finesse ring-down (RD) cavities. The two RD cavities are 1.0 and 1.4 m long, with finesse of 63000 and 131000, which results in effective path lengths of 20 km and 59 km for Hefei and Grenoble setups. The acousto-optic modulators (AOMs) are used

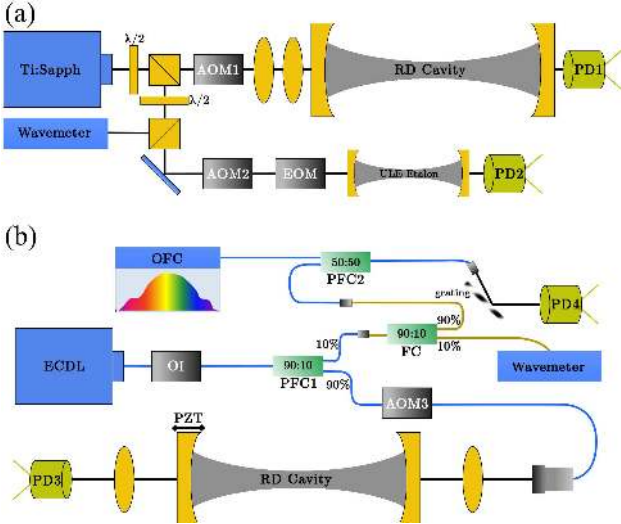


FIG. 1. Cavity ring-down spectrometers in Hefei (a) and Grenoble (b) laboratories. AOM - acousto-optic modulator, ECDL - external cavity diode laser, EOM - electro-optic modulator, FC - fiber coupler, OFC - optical frequency comb, OI - optical isolator, PD - photodiode, PFC - polarization fiber coupler, PZT - piezoelectric transducer, Ti:Sapph - Ti:sapphire laser.

as optical switches to generate the RD events. The frequency of the Hefei laser source (Ti:sapph) is set by a temperature-stabilized ( $\Delta T \approx 10$  mK at 302 K) ultralow expansion (ULE) etalon reaching 10 MHz accuracy (see Refs. [52, 53]), whereas for the Grenoble setup the external cavity diode laser (ECDL) is referenced to the optical frequency comb (OFC) reaching 300 kHz absolute accuracy (see Refs. [54–56]). The length of the Grenoble cavity is tunable with a piezoelectric actuator, which allows

the spectra to be recorded on a much denser frequency grid. The temperatures of the cavities were controlled to within 1 K and 0.15 K for the Hefei and Grenoble setups, respectively. For the 3-0 S(1) line, the H<sub>2</sub>/He mixing ratio spans between 33% and 10%, with 1% accuracy, while it has a constant value of 4.9(1)% for the 2-0 Q(1) line. The spectra were recorded at four pressures ranging from 0.36 to 1.35 atm with an accuracy of 0.5% and signal-to-noise ratio (SNR) up to 370 for the 3-0 S(1) line, as well as at nine pressures ranging from 0.07 to 1.05 atm with an accuracy of 0.15% and SNR up to 2800 for the 2-0 Q(1) line.

## III. AB INITIO CALCULATION OF THE COLLISIONAL EFFECTS

Our line-shape calculations [34, 35, 57, 58], originating from first principles, are based on the generalized Hess method (GHM) [37, 59, 60]. To better reproduce the physics of the velocity-changing collisions, we replace the commonly used hard-collision model [61, 62], which is used in GHM, with the model based on the Boltzmann operator for rigid-sphere approximation of the potential [9]. The latter model based on the isotropic part of the PES properly reproduces the dependence of the colliding partners on the mass ratio and describes the relation between velocities before and after collision [9], which is not the case for the simple hard-collision model. Moreover, we introduce the full speed dependence [63] of the collisional broadening and shift [60, 64, 65] into GHM.

For the H<sub>2</sub>-He system, the PES is three-dimensional; i.e., it depends on the distance between the center of mass of the hydrogen molecule and the helium atom,  $R$ , the intramolecular distance,  $r$ , and the angle between the inter- and intramolecular axes,  $\theta$ . To carry out the close-coupling quantum scattering calculations [66], the PES is projected on Legendre polynomials and averaged over the rovibrational wave functions of the hydrogen molecule [3, 32]. The generalized spectroscopic cross-sections,  $\sigma_{\lambda}^q$ , for the electric quadrupole lines considered here ( $q = 2$ ), as functions of the initial kinetic energy,  $E_{\text{KIN}}$ , are determined from S-matrix elements [32, 60, 64]. For the zero rank of the velocity tensor,  $\lambda = 0$ ,  $\sigma_{\lambda}^q$  reduces to the pressure broadening and shift cross-sections (PBXS and PSXS, respectively) [3, 65, 67, 68], while for  $\lambda = 1$  it provides the complex Dicke cross-section [31, 32, 59, 60, 64] (RDXS and IDXS for its real and imaginary parts, respectively). The resulting cross-sections are shown in Fig. 2, panels (a)-(d).

We use the generalized spectroscopic cross-sections to calculate the corresponding line-shape parameters at a given temperature  $T$ , i.e., the speed-dependent pressure broadening,  $\Gamma(v)$ , and shift,  $\Delta(v)$  [63, 69, 70], as well as

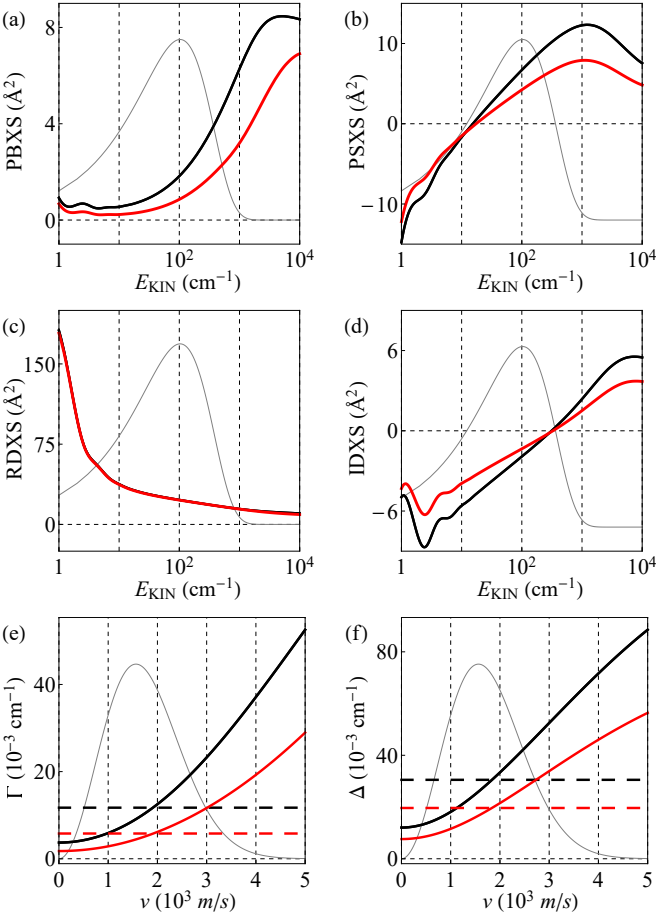


FIG. 2. (a-d) Generalized spectroscopic cross-sections for the 3-0 S(1) and 2-0 Q(1) lines in helium-perturbed H<sub>2</sub>: see the respective black and red lines, respectively. PBXS, PSXS, RDXS and IDXS are pressure broadening, pressure shift, and real and imaginary parts of complex Dicke cross-sections, respectively. The two curves in panel (c) are overlapping. (e, f) *Ab initio* speed dependence of the line broadening,  $\Gamma$ , and shift,  $\Delta$  (the same color notation), plotted for 1 amagat of He at the experimental temperatures. The black and red dashed lines are the speed-averaged collisional broadening,  $\Gamma_0$ , and shift,  $\Delta_0$ , respectively. The gray line is the Maxwell Boltzmann distribution at 296 K in arbitrary units; the distribution of relative kinetic energy in panels (a)-(d), and the distribution of active molecule speed in panels (e) and (f).

the complex Dicke parameter,  $\nu_{opt}$  [30, 39, 44, 71, 72]:

$$\Gamma(v) + i\Delta(v) = \left(\frac{n}{2\pi c}\right) \frac{2\tilde{v}_p^2}{v\sqrt{\pi}} \exp(-v^2/\tilde{v}_p^2) \times \times \int_0^\infty x^2 e^{-x^2} \sinh(2vx/\tilde{v}_p) \sigma_0^q(x\tilde{v}_p) dx, \quad (1a)$$

$$\nu_{opt} = \left(\frac{n}{2\pi c}\right) \frac{m_p}{m+m_p} \times \times \int_0^\infty v_r f_m(v_r) \left[ \frac{2}{3} \frac{v_r^2}{\bar{v}_r^2} \sigma_1^q(v_r) - \sigma_0^q(v_r) \right] dv_r, \quad (1b)$$

where  $v$ ,  $v_p$  and  $v_r$  are the speed of the active molecule, the speed of the perturber with the most probable value  $\tilde{v}_p = \sqrt{2k_B T/m_p}$ , and their relative speed with mean value  $\bar{v}_r$ , respectively, and  $x = v_r/\tilde{v}_p$ .  $m$ ,  $m_p$  and  $\mu$  are the masses of the active molecule and perturber and their reduced mass, respectively.  $f_m(v)$  is the Maxwell-Boltzmann speed distribution,  $n$  is the number density of the perturber,  $k_B$  is the Boltzmann constant and  $c$  is the speed of light. The *ab initio* speed-dependent broadenings and shifts are shown in Fig. 2, panels (e) and (f). The calculated line-shape parameters are gathered in Table I. We denote speed-averaged broadening and shift as  $\Gamma_0$  and  $\Delta_0$ , respectively: refer to the dashed horizontal lines in Fig. 2 (e) and (f). Following Ref. [35], we introduce two parameters,  $\Gamma_{SD} = \frac{v_m}{2} \frac{d\Gamma(v)}{dv}|_{v=\tilde{v}}$  and  $\Delta_{SD} = \frac{v_m}{2} \frac{d\Delta(v)}{dv}|_{v=\tilde{v}}$ , that quantify the strength of the speed dependence of the broadening and shift, respectively, where  $v_m$  is the most probable active molecule speed. The  $\Gamma_{SD}/\Gamma_0$  and  $\Delta_{SD}/\Delta_0$  ratios, larger than 0.4, reveal extraordinarily pronounced speed dependence for the H<sub>2</sub> case; for typical atmospheric systems, these ratios are at the level of 0.1 [73–75].

TABLE I. Calculated values of the line-shape parameters for the 3-0 S(1) and 2-0 Q(1) H<sub>2</sub> lines. The calculations are performed for  $T = 296.6 \text{ K}$  for the 3-0 S(1) line and for  $T = 294.2 \text{ K}$  for the 2-0 Q(1) line. All parameters are given in units of  $10^{-3} \text{ cm}^{-1}$  for  $n = 1$  amagat.

Line	$\Gamma_0$	$\Delta_0$	$\Gamma_{SD}$	$\Delta_{SD}$	$\nu_{opt}^r$	$\nu_{opt}^i$
3-0 S(1)	11.72	30.51	5.40	12.42	37.96	-17.45
2-0 Q(1)	5.74	19.51	2.68	8.06	41.64	-11.31

We calculate the He-perturbed shapes of the H<sub>2</sub> lines by averaging the velocity distribution of the optical coherence [33, 78, 79]

$$I(\omega) = \frac{1}{\pi} \Re e \int d^3 \vec{v} f_m(\vec{v}) h(\omega, \vec{v}). \quad (2)$$

$f_m(\vec{v})$  is the Maxwell-Boltzmann distribution of the active molecule velocity,  $\vec{v}$ , and  $f_m(\vec{v}) h(\omega, \vec{v})$  is a scalar function proportional to the velocity distribution of the optical coherence. The  $h(\omega, \vec{v})$  function fulfills the transport-relaxation equation [33, 79]

$$1 = -i(\omega - \omega_0 - \vec{k} \cdot \vec{v}) h(\omega, \vec{v}) - \hat{S}^f h(\omega, \vec{v}), \quad (3)$$

where  $\omega$  and  $\omega_0$  are the angular frequencies of the electromagnetic radiation and the unperturbed frequency of the molecular transition, respectively,  $\vec{k}$  is the wave vector and  $\hat{S}^f$  is the total collision operator describing relaxation and dephasing of the optical coherence as well as

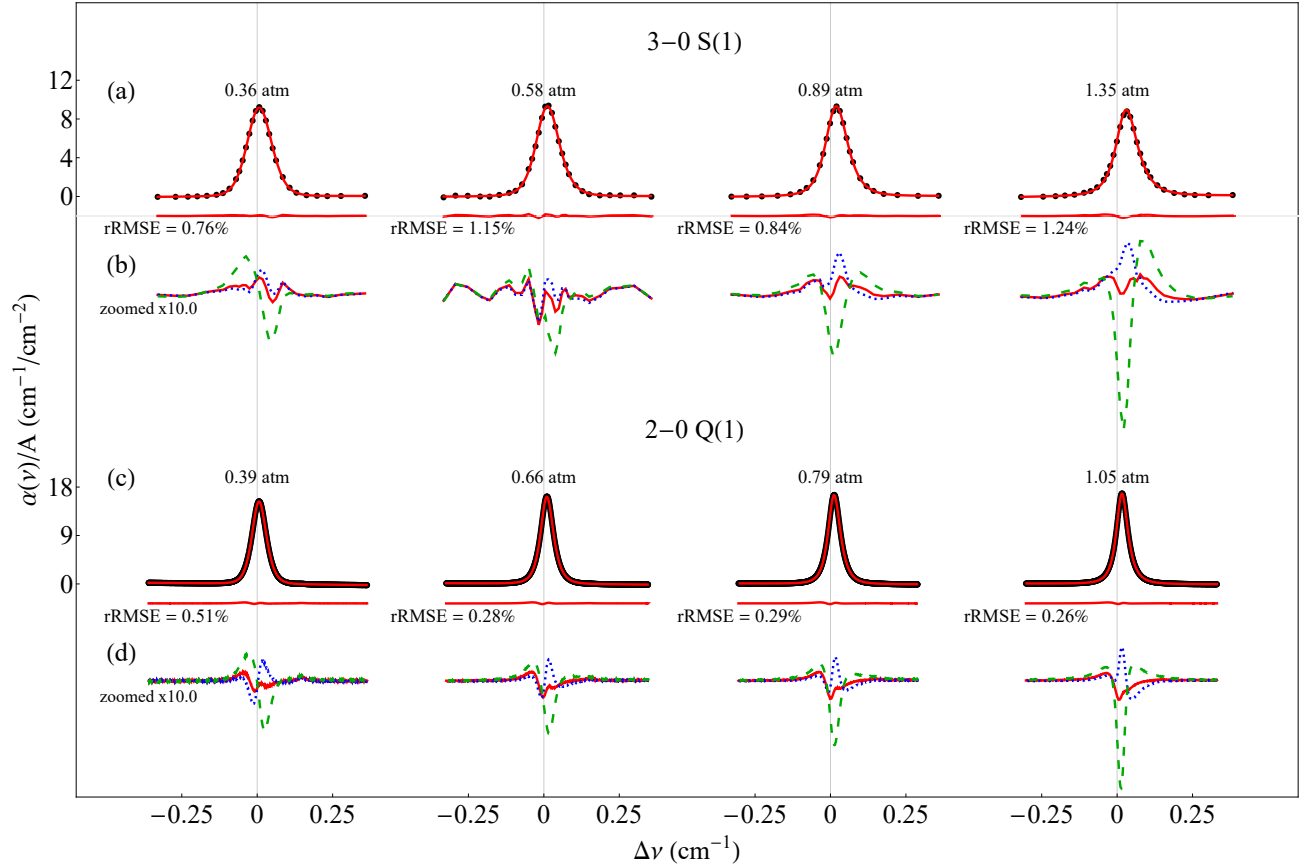


FIG. 3. Panels (a) and (c): Comparison of the raw experimental spectra (black points) and the simulated line profiles (red lines). The absorption axis has been normalized to the area of the spectral line,  $A$ . The red lines under the line profiles represent the differences between experiment and theory. rRMSE values on the plots describe the root-mean-square errors relative to the profile amplitude. Panels (b) and (d): The solid red, dotted blue and dashed green lines are the zoomed residuals for the BSP3 [30, 40], SK [38], and mMR [45, 46] potentials, respectively. The gray vertical lines indicate the theoretical unperturbed line position [76, 77]. The pressure shift is atypically large for  $\text{H}_2$  and despite small pressure range can be directly seen in this figure; see the deviation of the line maximum from the gray vertical line.

its flow between different velocity classes. This operator can be written as [34, 35, 57, 58]

$$\hat{S}^f = -\Gamma(v) - i\Delta(v) + \nu_{opt}\hat{M}_{BB}^f, \quad (4)$$

where  $\nu_{opt}\hat{M}_{BB}^f$  is the velocity-changing operator for the rigid-sphere model of collisions [80, 81]. By using the complex Dicke parameter derived from GHM,  $\nu_{opt}$ , we introduce the correlations between internal and translational degrees of freedom to the velocity-changing operator. The ultimate collision operator used to compare *ab initio* calculations with experiment is a sum of two contributions [9]: the  $\text{H}_2\text{-He}$  operator discussed here, Eq. (4), and the  $\text{H}_2\text{-H}_2$  operator taken from Ref. [82].

#### IV. EXPERIMENTAL VALIDATION OF THE QUANTUM SCATTERING CALCULATIONS AND TEST OF THE *AB INITIO* POTENTIALS

The direct comparison between theory and experiment is shown in Fig. 3, panels (a) and (c). Despite the fact that none of the line-shape parameters were fitted, we achieved subpercent agreement between the simulated and raw experimental profiles; i.e., the root-mean-square error of the *ab initio* model relative to profile amplitude (rRMSE) calculated within  $\pm\text{FWHM}$  is smaller than 1%. The pressure-average values of rRMSE are 0.99% and 0.33% for the 3-0 S(1) and 2-0 Q(1) lines, respectively. We do not know the reason why the discrepancy is larger for the 3-0 S(1) line. This is the first time that the fully *ab initio* line-shape calculations, including not only the collisional perturbations of both internal and translational motions of molecules but also the correlations between them, are validated for highly accurate experimental spectra. In addition to the line-shape

parameters, whose values are directly taken from our *ab initio* calculations, several other parameters (not related to the collisional effects) were fitted: the unperturbed line position frequency,  $\nu_0 = \omega_0/2\pi$ , the line intensity,  $S$ , and the background slope and baseline. The fitted values of  $\nu_0$  and  $S$  are consistent with the theoretical values [51, 76, 77] within the declared  $1\sigma$  uncertainties.

The advantage of the method employed in this work is that it allows the absolute value of the collisional cross-sections to be accurately tested experimentally, which is not the case for most of the other experimental techniques [16–18]. As an example, we consider the pressure broadening cross-section (PBXS in Fig. 2 panel (a)), which gives the  $\Gamma_0$  parameter after thermal averaging: refer to the dashed horizontal lines in Fig. 2 (e). At high pressures (at which the collisional broadening dominates), the relative error of  $\Gamma_0$  is approximately equal to the residual rRMSE. For instance, in the case of the 2-0 Q(1) line, rRMSE = 0.18% at the highest pressure corresponds to subpercent agreement between our *ab initio* and experimental values of  $\Gamma_0$ .

In addition to demonstrating that the full theoretical methodology can reproduce the collision-perturbed experimental profiles at an unprecedented level of accuracy, we show that this approach can serve as a link between high-precision spectroscopy and quantum chemical calculations, thus enabling experimental tests of PESs in regions that are inaccessible with other techniques. In Figure 3, panels (b) and (d), we show the differences between the experimental and theoretical profiles for three different PESs: the Schaefer and Köhler (SK) PES [38], modified Muchnik and Russek (mMR) PES [45, 46], and the PES used in our main analysis, namely the extended Bakr, Smith and Patkowski (BSP3) [30, 40]. Contrary to the main analysis here we do not fit the line intensity but fix it to the theoretical value [51]. We do so because for the older less accurate PESs [38, 45, 46] the fitted line intensities, to some extent, artificially compensate inaccurate values of some of the line-shape parameters. This comparison clearly demonstrates that the best agreement with the experiment is achieved for the BSP3 PES. This result is consistent with our expectations, since the most recent BSP3 surface was calculated using the coupled-cluster method with single, double and perturbative triple excitations (CCSD(T)), augmented by full configuration interaction corrections for which the relative uncertainty in the minimum is estimated as 0.4% ( $\pm 0.045 \text{ cm}^{-1}$ ). Two other potentials studied here, SK and mMR, were obtained using much smaller Gaussian basis sets and lower levels of electronic structure theory. Moreover, the BSP3 PES involves a consistent treatment of a large range of intramolecular H-H distances and ensures a proper asymptotic behavior for large H<sub>2</sub>-He separations [30].

## V. CONCLUSION

We demonstrated for the first time that the calculations from first principles are able to reproduce the experimental collision-perturbed molecular spectra at sub-percent level accuracy. We used quantum scattering calculations to construct a collision operator that describes not only the dephasing and damping of the optical coherence but also flows of an optical coherence between different velocity classes. We solved a Boltzmann-like transport-relaxation equation to determine the velocity distribution of optical coherence and, hence, the collision-perturbed shapes of molecular lines. The calculations were validated on the highly accurate experimental spectra of the H<sub>2</sub> S(1) 3-0 and Q(1) 2-0 electric quadrupole transitions perturbed by helium. In addition to validating the theoretical methodology of accurate determination of the collision-induced shapes of molecular lines, we demonstrated that this approach can be used to test the quantum-chemical calculations of the potential energy surfaces. This work demonstrates that theoretical calculations are capable of delivering line-shape parameters with the accuracy necessary to interpret experimental spectra for atmospheric, planetary, and astrophysical applications. With this approach, we show the possibility of calculating and validating beyond-Voigt line-shape parameters in order to populate line-by-line spectroscopic databases such as HITRAN [41], GEISA [42], or ExoMol [43] with requested accuracies in a wide temperature range for recent advanced database structures [44]. Such approach is important for the lines relevant for atmospheric and astrophysical applications, especially for those which have not been accessed yet with laboratory experiments.

## ACKNOWLEDGMENTS

M.S. contribution is supported by the Polish National Science Centre Project No. 2017/26/D/ST2/00371 and by the *A next-generation worldwide quantum sensor network with optical atomic clocks* project carried out within the TEAM IV Programme of the Foundation for Polish Science cofinanced by the European Union under the European Regional Development Fund. P.W. and H.J. contributions are supported by the Polish National Science Centre Project Nos. 2015/19/D/ST2/02195 and 2018/31/B/ST2/00720. S.-M.H. acknowledges the support from National Natural Science Foundation of China (21688102). M.K. and D.L. contributions are supported by the Polish National Science Centre Projekt No. 2015/18/E/ST2/00585. K.P. is supported by the U.S. National Science Foundation CAREER award CHE-1351978. P.Ż. contribution is supported by the Polish National Science Centre Project No. 2015/19/B/ST4/02707. The project is co-financed by the Polish National Agency for Academic Exchange under the PHC Polonium program (dec.

PPN/X/PS/318/2018). The research is part of the program of the National Laboratory FAMO in Toruń,

Poland. It is also supported by the COST Action CM1405 MOLIM.

- 
- [1] G. Herzberg and L. L. Howe, Can. J. Phys. **37**, 636 (1959).
- [2] A. Einstein and O. Stern, Ann. Phys. **40**, 551 (1913).
- [3] F. Thibault, P. Wcisło, and R. Ciuryło, Eur. Phys. J. D **70**, 236 (2016).
- [4] V. G. Cooper, A. D. May, E. H. Hara, and H. F. P. Knapp, Can. J. Phys. **46**, 2019 (1968).
- [5] P. Wcisło, F. Thibault, H. Cybulski, and R. Ciuryło, Phys. Rev. A **91**, 052505 (2015).
- [6] R. L. Farrow, L. A. Rahn, G. O. Sitz, and G. J. Rosasco, Phys. Rev. Lett. **63**, 746 (1989).
- [7] F. Chauvard, X. Michaut, R. Saint-Loup, H. Berger, P. Joubert, B. Lance, J. Bonamy, and D. Robert, J. Chem. Phys. **112**, 158 (2000).
- [8] H. Tran, F. Thibault, and J.-M. Hartmann, J. Quant. Spectrosc. Radiat. Transf. **112**, 1035 (2011).
- [9] P. Wcisło, H. Tran, S. Kassi, A. Campargue, F. Thibault, and R. Ciuryło, J. Chem. Phys. **141**, 074301 (2014).
- [10] S. G. Rautian and A. M. Shalagin, *Kinetic problems of non-linear spectroscopy* (North-Holland, Amsterdam, 1991).
- [11] F. R. W. McCourt, J. J. M. Beenakker, W. E. Köhler, and I. Kuscer, *Nonequilibrium Phenomena in Polyatomic Gases* (Oxford, Clarendon, 1991).
- [12] A. R. W. McKellar, J. Chem. Phys. **92**, 3261 (1990).
- [13] A. R. W. McKellar and J. Schaefer, J. Chem. Phys. **95**, 3081 (1991).
- [14] A. R. W. McKellar, J. Chem. Phys. **105**, 2628 (1996).
- [15] G. D. Sheldon, S. H. Fakhr-Eslam, P. M. Sinclair, J. R. Drummond, and A. D. May, Can. J. Phys. **79**, 173 (2001).
- [16] W. E. Perreault, N. Mukherjee, and R. N. Zare, Science **358**, 356 (2017).
- [17] W. E. Perreault, N. Mukherjee, and R. N. Zare, Nat. Chem. **10**, 561 (2018).
- [18] W. E. Perreault, N. Mukherjee, and R. N. Zare, J. Chem. Phys. **150**, 174301 (2019).
- [19] J. F. E. Croft, N. Balakrishnan, M. Huang, and H. Guo, Phys. Rev. Lett. **121**, 113401 (2018).
- [20] K. V. D. Hout, P. Hermans, E. Mazur, and H. Knaap, Physica A **104**, 509 (1980).
- [21] S. L. Bragg, W. H. Smith, and J. W. Brault, Astrophys. J. **263**, 999 (1982).
- [22] W. K. Bischel and M. J. Dyer, Phys. Rev. A **33**, 3113 (1986).
- [23] L. A. Rahn and G. J. Rosasco, Phys. Rev. A **41**, 3698 (1990).
- [24] L. A. Rahn, R. L. Farrow, and G. J. Rosasco, Phys. Rev. A **43**, 6075 (1991).
- [25] J. W. Forsman, J. Bonamy, D. Robert, J. P. Berger, R. Saint-Loup, and H. Berger, Phys. Rev. A **52**, 2652 (1995).
- [26] P. M. Sinclair, J. P. Berger, X. Michaut, R. Saint-Loup, R. Chaux, H. Berger, J. Bonamy, and D. Robert, Phys. Rev. A **54**, 402 (1996).
- [27] P. Hermans, A. V. Die, H. Knaap, and J. Beenakker, Physica A **132**, 233 (1985).
- [28] R. Blackmore, S. Green, and L. Monchick, J. Chem. Phys. **91**, 3846 (1989).
- [29] X. Michaut, R. Saint-Loup, H. Berger, M. L. Dubernet, P. Joubert, and J. Bonamy, J. Chem. Phys. **109**, 951 (1998).
- [30] F. Thibault, K. Patkowski, P. S. Żuchowski, H. Jóźwiak, R. Ciuryło, and P. Wcisło, J. Quant. Spectrosc. Radiat. Transf. **202**, 308 (2017).
- [31] R. Z. Martínez, D. Bermejo, F. Thibault, and P. Wcisło, J. Raman. Spectrosc. **49**, 1339 (2018).
- [32] H. Jóźwiak, F. Thibault, N. Stolarszyk, and P. Wcisło, J. Quant. Spectrosc. Radiat. Transf. **219**, 313 (2018).
- [33] R. Blackmore, J. Chem. Phys. **87**, 791 (1987).
- [34] R. Ciuryło, D. A. Shapiro, J. R. Drummond, and A. D. May, Phys. Rev. A **65**, 012502 (2002).
- [35] P. Wcisło, F. Thibault, M. Zaborowski, S. Wójciewicz, A. Cygan, G. Kowzan, P. Masłowski, J. Komasa, M. Puchalski, K. Pachucki, R. Ciuryło, and D. Lisak, J. Quant. Spectrosc. Radiat. Transf. **213**, 41 (2018).
- [36] A. May, W.-K. Liu, F. McCourt, R. Ciuryło, J. S.-F. Stoker, D. Shapiro, and R. Wehr, Can. J. Phys. **91**, 879 (2013).
- [37] S. Hess, Physica **61**, 80 (1972).
- [38] J. Schaefer and W. Köhler, Physica A **129**, 469 (1985).
- [39] L. Demeio, S. Green, and L. Monchick, J. Chem. Phys. **102**, 9160 (1995).
- [40] B. W. Bakr, D. G. A. Smith, and K. Patkowski, J. Chem. Phys. **139**, 144305 (2013).
- [41] I. E. Gordon, L. S. Rothman, C. Hill, R. V. Kochanov, Y. Tan, P. F. Bernath, M. Birk, V. Boudon, A. Campargue, K. V. Chance, B. J. Drouin, J.-M. Flaud, R. R. Gamache, J. T. Hodges, D. Jacquemart, V. I. Perevalov, A. Perrin, K. P. Shine, M.-A. H. Smith, J. Tennyson, G. C. Toon, H. Tran, V. G. Tyuterev, A. Barbe, A. G. Császár, V. M. Devi, T. Furtenbacher, J. J. Harrison, J.-M. Hartmann, A. Jolly, T. J. Johnson, T. Karman, I. Kleiner, A. A. Kyuberis, J. Loos, O. M. Lyulin, S. T. Massie, S. N. Mikhailenko, N. Moazzen-Ahmadi, H. S. P. Müller, O. V. Naumenko, A. V. Nikitin, O. L. Polyansky, M. Rey, M. Rotger, S. W. Sharpe, K. Sung, E. Starikova, S. A. Tashkun, J. V. Auwera, G. Wagner, J. Wilzewski, P. Wcisło, S. Yu, and E. Zak, J. Quant. Spectrosc. Radiat. Transf. **203**, 3 (2017).
- [42] N. Jacquinot-Husson, R. Armante, N. Scott, A. Chédin, L. Crépeau, C. Boutammine, A. Bouhdaoui, C. Crevoisier, V. Capelle, C. Boonne, N. Poulet-Crovisier, A. Barbe, D. C. Benner, V. Boudon, L. Brown, J. Buldyreva, A. Campargue, L. Coudert, V. Devi, M. Down, B. Drouin, A. Fayt, C. Fittschen, J.-M. Flaud, R. Gamache, J. Harrison, C. Hill, Ø. Hodnebrog, S.-M. Hu, D. Jacquemart, A. Jolly, E. Jiménez, N. Lavrentieva, A.-W. Liu, L. Lodi, O. Lyulin, S. Massie, S. Mikhailenko, H. Müller, O. Naumenko, A. Nikitin, C. Nielsen, J. Orphal, V. Perevalov, A. Perrin, E. Polovtseva, A. Predoi-Cross, M. Rotger, A. Ruth, S. Yu, K. Sung, S. Tashkun, J. Tennyson, V. Tyuterev, J. V. Auwera, B. Voronin, and A. Makie, Journal of

- Molecular Spectroscopy **327**, 31 (2016).
- [43] J. Tennyson, S. N. Yurchenko, A. F. Al-Refaie, E. J. Barton, K. L. Chubb, P. A. Coles, S. Diamantopoulou, M. N. Gorman, C. Hill, A. Z. Lam, L. Lodi, L. K. McKemmish, Y. Na, A. Owens, O. L. Polyansky, T. Rivlin, C. Sousa-Silva, D. S. Underwood, A. Yachmenev, and E. Žak, *J. Mol. Spectrosc.* **327**, 73 (2016).
- [44] N. Stolarczyk, F. Thibault, H. Cybulski, H. Jóźwiak, G. Kowzan, B. Vispoel, I. Gordon, L. Rothman, R. Gamache, and P. Wcisło, *J. Quant. Spectrosc. Radiat. Transf.* **240**, 106676 (2020).
- [45] A. I. Boothroyd, P. G. Martin, and M. R. Peterson, *J. Chem. Phys.* **119**, 3187 (2003).
- [46] P. Muchnick and A. Russek, *J. Chem. Phys.* **100**, 4336 (1994).
- [47] Y. Tan, J. Wang, C.-F. Cheng, X.-Q. Zhao, A.-W. Liu, and S.-M. Hu, *J. Mol. Spectrosc.* **300**, 60 (2014).
- [48] D. Romanini, A. Kachanov, N. Sadeghi, and F. Stoeckel, *Chem. Phys. Lett.* **264**, 316 (1997).
- [49] P. Macko, D. Romanini, S. Mikhailenko, O. Naumenko, S. Kassi, A. Jenouvrier, V. Tyuterev, and A. Campargue, *J. Mol. Spectrosc.* **227**, 90 (2004).
- [50] S. Kassi and A. Campargue, *J. Chem. Phys.* **137**, 234201 (2012).
- [51] A. Campargue, S. Kassi, K. Pachucki, and J. Komasa, *Phys. Chem. Chem. Phys.* **14**, 802 (2012).
- [52] C.-F. Cheng, Y. R. Sun, H. Pan, J. Wang, A.-W. Liu, A. Campargue, and S.-M. Hu, *Phys. Rev. A* **85**, 024501 (2012).
- [53] C.-F. Cheng, Y. R. Sun, H. Pan, Y. Lu, X.-F. Li, J. Wang, A.-W. Liu, and S.-M. Hu, *Opt. Express* **20**, 9956 (2012).
- [54] D. Mondelain, S. Kassi, T. Sala, D. Romanini, D. Gatti, and A. Campargue, *J. Mol. Spectrosc.* **326**, 5 (2016).
- [55] D. Mondelain, S. Mikhailenko, E. Karlovets, S. Béguier, S. Kassi, and A. Campargue, *J. Quant. Spectrosc. Radiat. Transf.* **203**, 206 (2017).
- [56] S. Mikhailenko, D. Mondelain, E. Karlovets, S. Kassi, and A. Campargue, *J. Quant. Spectrosc. Radiat. Transf.* **206**, 163 (2018).
- [57] R. Ciuryło, A. Bielski, J. R. Drummond, D. Lisak, A. D. May, A. S. Pine, D. A. Shapiro, J. Szudy, and R. S. Trawiński, in *AIP Conf. Proc.* (AIP, 2002).
- [58] D. Lisak, J. T. Hodges, and R. Ciuryło, *Phys. Rev. A* **73**, 012507 (2006).
- [59] G. C. Corey and F. R. McCourt, *J. Chem. Phys.* **81**, 2318 (1984).
- [60] L. Monchick and L. W. Hunter, *J. Chem. Phys.* **85**, 713 (1986).
- [61] M. Nelkin and A. Ghatak, *Phys. Rev.* **135**, A4 (1964).
- [62] S. G. Rautian and I. I. Sobelman, *Sov. Phys. Usp.* **9**, 701 (1967).
- [63] P. R. Berman, *J. Quant. Spectrosc. Radiat. Transf.* **12**, 1331 (1972).
- [64] J. Schaefer and L. Monchick, *J. Chem. Phys.* **87**, 171 (1987).
- [65] R. Shafer and R. G. Gordon, *J. Chem. Phys.* **58**, 5422 (1973).
- [66] J. M. Hutson and S. Green, Molscat computer code, version 14, distributed by Collaborative Computational Project No. 6 of the UK Science and Engineering Research Council (1994).
- [67] A. Ben-Reuven, *Phys. Rev.* **141**, 34 (1966).
- [68] A. Ben-Reuven, *Phys. Rev.* **145**, 7 (1966).
- [69] H. M. Pickett, *J. Chem. Phys.* **73**, 6090 (1980).
- [70] A. Pine, *J. Quant. Spectrosc. Radiat. Transf.* **62**, 397 (1999).
- [71] J. Schaefer and L. Monchick, *Astron. Astrophys.* **265**, 859 (1992).
- [72] G. Kowzan, P. Wcisło, M. Słowiński, P. Maśłowski, A. Viel, and F. Thibault, *J. Quant. Spectrosc. Radiat. Transf.* **243**, 106803 (2020).
- [73] M. Ghysels, Q. Liu, A. J. Fleisher, and J. T. Hodges, *Appl. Phys. B* **123**, 124 (2017).
- [74] M. Konefal, S. Kassi, D. Mondelain, and A. Campargue, *J. Quant. Spectrosc. Radiat. Transf.* **241**, 106653 (2020).
- [75] J. Domyslawska, S. Wójciewicz, P. Maśłowski, K. Bielska, A. Cygan, M. Słowiński, R. S. Trawiński, R. Ciuryło, and D. Lisak, *J. Quant. Spectrosc. Radiat. Transf.* **242**, 106789 (2020).
- [76] J. Komasa, K. Piszczałkowski, G. Lach, M. Przybytek, B. Jeziorski, and K. Pachucki, *J. Chem. Theory Comput.* **7**, 3105 (2011).
- [77] P. Czachorowski, M. Puchalski, J. Komasa, and K. Pachucki, *Phys. Rev. A* **98**, 052506 (2018).
- [78] A. D. May, *Phys. Rev. A* **59**, 3495 (1999).
- [79] D. A. Shapiro, R. Ciuryło, J. R. Drummond, and A. D. May, *Phys. Rev. A* **65**, 012501 (2002).
- [80] M. J. Lindenfeld, *J. Chem. Phys.* **73**, 5817 (1980).
- [81] P. F. Liao, J. E. Bjorkholm, and P. R. Berman, *Phys. Rev. A* **21**, 1927 (1980).
- [82] P. Wcisło, I. E. Gordon, H. Tran, Y. Tan, S.-M. Hu, A. Campargue, S. Kassi, D. Romanini, C. Hill, R. V. Kochanov, and L. S. Rothman, *J. Quant. Spectrosc. Radiat. Transf.* **177**, 75 (2016).